Finite size effects in simulations of thermal conductivity under lower mantle conditions

Ben Todd,* Stephen Stackhouse, Andrew M. Walker, and Jon E. Mound

School of Earth and Environment, University of Leeds, United Kingdom

(Dated: November 10, 2017)

Abstract

Knowledge of thermal conductivity is important for modelling the deep earth, but can not be measured experimentally at core mantle boundary conditions. Atomic scale simulations sidestep experimental limitations, but system size must be chosen carefully in order to determine accurate conductivity values.

Here we investigate the effects of finite simulation size and show how conductivity can be overestimated when using the direct method. EXTRAPOLATION PROCEDURE

Classical molecular dynamics approaches are utilised, with the intention of constraining system parameters for future ab-initio studies.

RESULTS

* Corresponding author: ee10bt@leeds.ac.uk

I. INTRODUCTION

A. Intro Intro (remove this subsection header later)

A range of atomic scale simulation methods are available to determine the thermal conductivity of materials, which are invaluable in situations where experiments are difficult. An example of extreme conditions is the Earth's lower mantle, where pressures and temperatures reach around 136 GPa and 4000 K above the core-mantle boundary (CMB). Many studies assume lowermost mantle thermal conductivity to be 10 $Wm^{-1}K^{-1}$ (Lay *et al.* [1]), but uncertainty in the extrapolation of low pressure and/or temperature experiments gives a range of 4 - 16 $Wm^{-1}K^{-1}$ (Brown and McQueen [2], Osako and Ito [3], Hofmeister [4], Goncharov *et al.* [5], Manthilake *et al.* [6], Ohta *et al.* [7]).

B. Pre-intro to methods (remove this subsection header later)

Stackhouse and Stixrude [8] give a review of different methods to compute thermal conductivity, in the present work we focus on two methods: (1) Equilibrium molecular dynamics utilising the Green-Kubo relations to determine the thermal conductivity from heat flux fluctuations and their time-dependence (Green [9], Kubo [10, 11], Schelling *et al.* [12]). (2) The "direct method" utilising non-equilbrium molecular dynamics, where thermal conductivity relates to an imposed heat flux and resultant temperature gradient via Fourier's Law [Muller-Plathe [13], Nieto-Draghi and Avalos [14]]

C. The question/motivation (remove this subsection header later)

Considering systems of varying size, length-dependent conductivities are obtained from the direct method and extrapolated to the bulk material (Schelling *et al.* [12]). The validity of this extrapolation procedure have been called into question (e.g. Sellan *et al.* [15]), when a linear trend cannot be fit through the length-dependent conductivities. Herein we describe three finite-size effects (FSE) which cause the conductivity result of a simulation to diverge from the value expected by a linear trend, and offer a comparison with results obtained from the Green-Kubo method. THIS PARA MAY BE MORE IMPORTANT IN ABSTRACT

D. Bridgmanite (remove this subsection header later)

Bridgmanite, or [$MgSiO_3$/magnesium silicate] perovskite, comprises around 80% (75%? REF?) of the lower mantle (need to mention the other 20%?), and is an insulator past its Debye temperature at all conditions relevant to the deep earth (TRUE? REF?). There have been several computational studies to calculate the lattice thermal conductivity of bridgmanite at CMB conditions. Our approach will be very similar to that of Ammann *et al.* [16], who use the direct method and interatomic potentials to produce a value of $\sim$8.5 $Wm^{-1}K^{-1}$. Stackhouse *et al.* [17] again use the direct method but with density functional theory, yielding conductivity of 6.8 ± 0.9 $Wm^{-1}K^{-1}$. Using Green-Kubo, Haigis [18] report a value of 12.4 ± 2.0 $Wm^{-1}K^{-1}$for conditions of 3000 K, 139 GPa. Tang *et al.* [19] and Dekura *et al.* [20] employ first principles, anharmonic lattice dynamics techniques, respectively obtaining values of $\sim$1 $Wm^{-1}K^{-1}$(CMB conditions) and 2.3 $Wm^{-1}K^{-1}$(for 4000 K and 100 GPa).

E. Intro to rest of paper (remove this subsection header later)

In section II (Section?) we provide an overview of the methods and expand on issues. In section III we outline our computational approaches, for the non-equilibrium molecular dynamics direct method and equilibrium molecular dynamics Green-Kubo method. The two methods have previously been compared (e.g. Schelling *et al.* [12]), and have been found to give results in good agreement. In section IV we show convergence of computed conductivity with respect to simulation cell size and shape (AND PRESSURE/TEMPERATURE EFFECTS?). ALSO IN RESULTS, DISCUSS SCALING LAW / THEORETICAL MODEL? In section V we suggest the minimum system parameters to be utilised in similar lower mantle studies, and discuss potential future work.

II. THEORY

A. Phonons (remove this subsection header later???)

PHYSICS JOURNAL LEVEL? A fundamental concept in atomic scale simulations of thermal conductivity, heat is (CAN BE?) transported as lattice virbrations, or phonons (MENTION RADIATIVE/ELECTRICAL? MENTION HOW WE DON'T CARE ABOUT

EITHER FOR BRIDG HERE?). The further phonons travel before scattering (mean free path, MFP) the more efficient the heat transport, and thus the higher the thermal condutivity. A number of effects (MATTHIESSEN'S RULE) cause phonons to scatter: (1) collisions with other phonons in the lattice, (2) boundaries or defects in the material, and (3) impurities in the atomic structure (ALSO ELECTRONS?). The finite-size effects we describe are associated with (1), where simulation system sizes are too small to recreate the phonon-phonon scattering of the bulk material. The FSE observed for a material will change with thermal conductivity/phonon MFP, and thus are pressure, temperature, and composition sensitive. Higher conductivity materials/conditions require larger systems to eliminate FSE (and vice versa) [[[BUT IS THIS TRUE? SHOULD IT BE IN THIS SECTION, OR DISCUSSION?]]]

B. Direct method (remove this subsection header later???)

The direct method is the computational implementation of a typical experiment to measure thermal conductivity, using Fourier's law to relate heat flux (q) and temperature gradient (∇T) to thermal conductivity (k),

$$q = -k\nabla T. \tag{1}$$

In the direct method energy is transferred from one group of atoms to another, creating hot and cold regions between which heat flows. The resultant temperature gradient is measured by calculating the temperature of individual groups of atoms along the direction of the heat flux. Simulation cells tend to be long relative to their cross-sectional area, defined as height by width. In this study (SHOULDN'T BE TALKING SPECIFIC AT THIS POINT?) cell boundaries are periodic and the hot and cold sections are half the cell length apart, meaning heat flows out of both ends of the cell from hot to cold. This results in two similar temperature gradients which can be averaged.

From kinetic theory REFERENCE, conductivities computed by the direct method (k_L) are dependent on length of simulation cell,

$$k_L = \frac{1}{3} C_V v l_L, \tag{2}$$

where C_v is the volumetric heat capacity, v is the BULK SOUND VELOCITY?, and l_L is the phonon mean free path. The finite size of the simulation cell truncates the mean free path, underestimating conductivity compared to that of the bulk material (k_∞). Using results from simulations of varying cell length (L), conductivity is extrapolated to a length-independent value (where b is a material dependent parameter),

$$k_L{}^{-1} = bL^{-1} + k_\infty{}^{-1}. \tag{3}$$

Inverse conductivities from direct method simulations are plotted against corresponding inverse cell lengths. A straight line is fit to the data and extrapolated to the y-axis (at which the inverse cell length equals zero and real length equals infinity), where the intercept gives the inverse of the bulk material conductivity, see Figure **??**(REFERENCE SCHELLING HERE?).

Problems arise when the data don't support a linear trend. There are two effects of finite system size available that cause an individual direct method simulation to diverge away from the inferred linear trend, both of which resulting in overestimations of the length dependent conductivity. Firstly, when the distance between hot and cold sections is shorter than the MFP, phonons travel ballistically (i.e. without any scattering events) from heat source to sink (Sellan *et al.* [15]). These overestimations occur to the right of the expected linear region on the inverse conductivity/length plots, reducing the gradient of the linear fit and underestimating the extrapolated conductivity.

Secondly, for a fixed cross-sectional area, as cell length tends to infinity so does conductivity ([21]). This effect is due to relatively sparse phonon phase sampling in the cross-section compared to length (PHONONS THAT AREN'T RESOLVED CAN'T CONTRIBUTE TO PHONON-PHONON SCATTERING), and can be observed on the inverse plot where long cells exhibit increasing conductivity away from the linear region. Unlike above, this divergence causes the gradient of a linear fit to increase and an overestimation to extrapolated conductivity. By comparing results with the Green-Kubo method, we will constrain the cell lengths in the linear extrapolation region to mitigate these effects. INCREASING CSA DOES NOT SUFFICIENTLY REDUCE THIS EFFECT

A third effect of system size can cause an incorrect conductivity extrapolation, when the cross-sectional area is too small (Thomas *et al.* [22]? NANOTUBE DIAMETER RATHER THAN CSA). The effect of phonon-phonon scattering is underestimated in small area systems due to a restriction of the active phonon modes. Reduced scattering means heat transport is artificially more efficient than expected from the bulk material. The general effect of this on the inverse conductivity/length plot is a systematic shift of data towards higher conductivities. We will investigate this effect by varying CSA for a range of cell lengths, extrapolated conductivity will decrease with CSA until it reaches a converged value. We will use the smallest area that produces the converged conductivity for computational efficiency.

C. Green-Kubo method (remove this subsection header later???)

REDUNDANCY WITH METHODOLOGY

The Green-Kubo method uses auto-correlation functions (ACFs) to quantify time-dependence of heat fluxes (shown in Figure **??**, and Equation 4), in a simulation cell of roughly cubic dimensions and spatially-consistent average temperature. Instantaneous heat fluxes can be used to determine how energy is dissipated within a system, where brief flux events mean heat is transferred quickly indicating high thermal conductivity (and vice versa). Auto-correlation is performed over the net heat flux series in each crystallographic direction, for a timescale up to a user-specified correlation length.

$$ACF_i = \langle J_i(0) \cdot J_i(t) \rangle \,, \tag{4}$$

where i specifies crystallographic axis, J is heat flux, and t is the correlation length. The integral of heat flux ACF is proportional to thermal conductivity via the Green-Kubo equation (see Figure **??** and Equation 5),

$$\kappa_i = \frac{V}{k_B T^2} \int_0^\infty \langle J_i(0) \cdot J_i(t) \rangle \, dt, \tag{5}$$

where V is the simulation cell volume, k_B is the Boltzmann constant, and T is the average temperature of the system. In this study we use Green-Kubo results as an independent check on the direct method, as they do not have the same finite size-effects. Obtaining a converged conductivity result simply depends on using a large enough cell volume / number of atoms.

The individual integrals obtained from the Green-Kubo show variation from the mean on the order of $\mathrm{Wm^{-1}K^{-1}}$. Many simulations from different intital temperature conditions are required in order to ensure good sampling of conductivity, as well as ensuring the computation time for each is long enough for convergence. This makes Green-Kubo a computationally expense method, especially for large systems.

STACKHOUSE 2010 REFERENCES Volz and Chen 2000; Sun and Murthy 2006

III. METHODOLOGY

ENOUGH INFO FOR REPRODUCIBILITY !!!

WHAT I HAVE DONE / FOR REPRODUCIBILITY. SETUP STUFF, BUT CONDUCTIVITY / FINITE SIZE EFFECT RESULTS GO IN RESULTS SECTION

Using the classical molecular dynamics code LAMMPS(Plimpton [23]) (Large-scale Atomic/Molecular Massively Parallel Simulator), we calculate lattice thermal conductivities and constrain effects of finite simulation size. With the interatomic potential of Oganov *et al.* [24] we simulate bridgmanite ($MgSiO_3$ perovskite), the predominant phase in the lower mantle ($\sim$75%).

To assess the finite-size effects within bridgmanite, we use larger simulation cells than those employed in previous studies. The atom counts associated with these cells (the largest cell considered having over 100,000 atoms) means an ab initio study would be impractical, necessitating the use of interatomic potentials. We expect the potentials to represent the finite size effects well, even if computed conductivities may inaccurate compared to first-principles calculations.

We present our approach for the direct and Green-Kubo methods, and show our calculations are converged with respect to simulation time and correlation length respectively. The finite-size effect analysis for both methods can be found in Section. IV, along with a results comparison.

A. Direct method

The simulation supercell is grouped into sections along its length, each half a unit cell wide. Two of these sections, half the supercell length apart, are designated as the heat source and sink. We measure the temperature in all sections to obtain the temperature gradient. This sets the minimum supercell length to 6 unit cells, in order for sufficient [statistics and resolution???] on the temperature gradient.

Heat flows in both directions away from the hot section because of cell periodicity, meaning there are two temperature gradients to average. Where L is supercell length in unit cells and S (= 2L) gives the number of sections, we obtain S/2 + 1 temperature points to fit the gradient. Because the temperature gradient is non-linear around the heat source and sink, we ignore S/12 sections (rounded to nearest integer) from both ends of the temperature gradient. For a given simulation cell we fit S/3 + 1 points to obtain the temperature gradient.

Changing the width of the heated sections has no effect on the conductivity result. Furthermore, changing the width (and thus number) of temperature bins has no effect on the sampled gradient, assuming resolution is large enough to capture the non-linear region around the heat source/sink.

An important criterion for utilising the direct method is that the temperature gradient is sensible, too large a range between hot and cold sections means Fourier's law becomes invalid. Additionally thermal conductivity is strongly temperature-dependent at upper lower-mantle conditions (1000 K), it is therefore undesirable to have substanially different conductivities as a of function of temperature across the cell. The opposite case is also true, the difference in temperature between hot and cold sections must be larger than the uncertainty in the average system temperature.

We typically observe fluctuations in temperature of around ±50 K during temperature equilibration, and look for temperature increases/decreases on the order of 10% the mean temperature. We control the magnitude of the gradient by altering the interval at which heat is exchanged. To produce the desired gradients we find shorter intervals are required as cell length decreases, cross-sectional area increases, and system equilibrium temperature decreases.

We ensure all calculations are run for a sufficient length of time for the conductivity value to converge (see Figure **??**). When conductivity fails to converge it means either the simulations needs to be run for longer (unlikely with our nanosecond-scale classical calculations), or the system temperature has drifted. When NVE simulations are run for a long time there is noticable drift in the average system temperature (due to numerical approximations in the equation of motion), which in turn causes drift in the computed conductivity.

B. Green-Kubo method

REDUNDANCY WITH THEORY SECTION

The bridgmanite unit cell does not have cell dimensions resembling a cube (a:b:c = 1:1:1.4), so we use supercell structures of 3x3x2, 4x4x3, 5x5x4, 6x6x4 etc. to make an approximately cubic simulation cell. Temperature initialisation (NVT) of 1 ns is run to ensure convergence of system pressure and temperature. To obtain heat flux auto-correlation functions, a simulation for each initial temperature condition is run for X ns, with 9 successive repeats for a total of 10 jobs. This gives 10 ACFs from each initial condition. Simulation runs are split in this manner to be feasible computationally, and also to provide enough samples for ensemble averaging statistics (???).

3x3x2 - X = 10 ns, for 20 inital conditions - 2 μs total time

4x4x3 - X = 10 ns, for 30 inital conditions - 3 μs total time

5x5x4 - X = 5 ns, for 20 inital conditions - 1 μs, X = 1 ns, for 70 inital conditions - 0.7 μs, 1.7 μs total time

6x6x4 - X = 1 ns, for 80 inital conditions - 0.8 μs total time

THIS INFO IN A TABLE, OR JUST GIVE FOR THE RELEVANT VOLUME?

In this study we compute ACFs up to correlation lengths of 100 ps, with 1 fs timesteps. This length is longer than required but selected as a proof of concept to show convergence in the conductivity result, additionally to display the extent and behaviour of drift in the integrals for long correlation times. We show in Figure **??** that the magnitude of the ACF decays to much less than 1% of its initial value around a correlation time of 1 ps, inferring the start of convergence for the integral and thus conductivity. (ACF FIGURE FOR CORREL ¡ 10PS?, RUNNING AVERAGE SHOWS CONVERGENCE)

(((ABOLISH THIS PARAGRAPH? MOVE HOWELL COMMENTS TO THEORY)))Figure **??** shows drift in the integral at long correlation lengths. The ACF should decay to zero as correlation time tends to infinity, however noise in the ACF prevents this. This will ultimately cause the integral to diverge on long timescales. Howell [25] fits a series of exponential decays to their ACF, forcing the expected decay to zero and subsequent (constant) integral convergence. This is represents a significant improvement on the conductivity estimate at long correlation lengths, but is mostly similar with the un-fit integrals early in the correlation. (INTEGRAL DRIFT FIGURE, JUST THE ONE INTEGRAL FOR 100PS)

ACFs produced by each simulation are integrated seperately, after which the integrals are averaged into a single series with uncertainty (standard deviation of the mean, **??**). This process is performed for heat fluxes in each crystallographic direction, allowing analysis of anisotropy and finite system size effects. We obtain a conductivity value from the combined integral by averaging a window between correlation times of 2-10 ps (for 136 GPa, 4000 K [THIS WILL NEED TO BE CHANGED]). Windows are chosen to capture a flat, converged region of the integral, or the section just after the 'bottleneck' if convergence is not obvious (**??**, but show window, and example of bottleneck?). We find correlation time of 2-10 ps to be long enough for good sampling of the integral, and short enough to ignore the aforementioned drift-effects. (INTEGRAL FIGURE WITH UNCERTAINTY FOR ¡10PS?, POINT TO CONVERGENCE, SHOW SMALL ZOOM OUT OF SAME GRAPH UP TO 100PS. SOME WAY TO COMBINE WITH ABOVE FIGURE)

AAARRGH!!! - CONVERGENCE OF KAPPA WITH SIMULATION TIME - AAARRGH!!!

DONT NEED ALL THESE GRAPHS

IV. RESULTS

LOTS OF QUANTIFYING

A. Green-Kubo method

A supercell volume of 3x3x2 (((REFER TO GRAPH, WILL NEED 1000K TOO))) fails to reproduce conductivities on the same order as the larger cells for all directions. We identify 4x4x3 and larger cells as being converged with respect to cell volume (((PROBLEMATIC STATEMENT, NOT CONVINCING, BY WHAT METRIC?))). This a useful result in terms of computation efficiency, as 6x6x4 supercells are 3 times as large (VOLUMOUS? REFERENCE ATOM COUNT?) as 4x4x3. Whereas here our error bars represent statistics on the integrals, the errors we take on results from 4x4x3 cells going forward will be related to the variation with the larger cells ((THIS IS OBVIOUS NONSENSE, HAVE TO CHANGE)).

These parameter choices are justified by comparison with Green Kubo results (Figure **??**), where the difference in computed conductivity is less than 0.4 W/m.K.

FINITE SIZE EFFECTS

B. Direct method

(((We consider FSE in the computed thermal conductivity at geophysically-relevant conditions of the CMB, but also consider the unphysical pressure/temperatures of 136 GPa and 1000 K.))) MFP DEPENDENT FSE, PROVE DIFFERENCE. BUT HAVEN'T DONE GK FSE AT 1000K! UPDATE - GK RUINS EVERYTHING

In addition to the expected conductivity increase with cell length, we observe two effects of finite system size.

Cells of length greater than 16 unit cells ($1/N < 0.0625$ on Figure **??**) show clear deviation from the expected linear trend.

As it is inappropriate to fit non-linear data, we ignore conductivity results from the long cells and perform the extrapolation only where a linear trend is suitable.

While the extrapolation procedure requires multiple cell lengths, the effects of cell cross-sectional area are not considered.

We show cells with small cross-section overestimate conductivity, the magnitude of which decreases with increasing area.

A sufficient cross-sectional area for bridgmanite is greater than 2x2, as extrapolated conductivities converge.

To obtain thermal conductivity results that are converged with respect to direct method system size, we use the following criteria,

Cell lengths $\leq$ 16 unit cells

Cross-section = 2x2 unit cells

SCALING LAW / THEORETICAL MODEL

YOU SHOULD DO YOUR FSE ANALYSIS AT LARGEST MFP CONDITION PAIR, HIGH P LOW T

PREVIOUS WORK :(

V. SUMMARY AND CONCLUSION

For bridgmanite, we show that use of the direct method for calculation of thermal conductivity will lead to an overestimate if the simulation cell is too long (>16 unit cells). Small cross-sectional areas (<2x2 unit cells) also overestimate the thermal conductivity. This informs future work using Density Functional Theory, and will allow a model of lower mantle conductivity considering composition to be established.

(ASSUMING THE RESULTS ARE CORRECT AND AGREE WITH GK) We see the non-linear region as described by Sellan *et al.* [15] for the cell length of 6 unit cells at 1000 K, which has individually higher conductivity than expected from the linear fit through data points corresponding to lengths of 8-16 unit cells. When included in the extrapolation, this reduces the gradient of the fit, raising the intercept and thus causing conductivity to be underestimated. At temperature of 4000 K, the 6 length cell is inline with the fit through other cells with length less than 16 unit cells. As the ratio of cell length to phonon MFP increases with temperature, we believe the onset of divergence as described by Sellan et al. moves to the right (??? - MENTION ACTUAL EFFECT - QUANTIFY RATHER THAN REFERENCING GRAPH). A shorter MFP needs shorter cell lengths to display divergent conductivity, of which we have not sampled (at high temperature). DOING THE DIRECT METHOD WITH CELLS OF LENGTH LESS THAN 6 UNIT CELLS AT ANY TEMPERATURE IS A BAD IDEA BECAUSE ...

(ASSUMING 8 LENGTH IS LONGER THE MFP AND NOT 24) We find conductivity is definitely dependent on CSA, but we were not able to increase CSA enough to eliminate aspect ratio-dependent divergence as reported by Hu *et al.* [21]. This does support our conclusion ignoring long cell lengths however, in order to keep the aspect ratio within a reasonable limit and ensure a linear fit is extrapolated. (EVEN THOUGH 48x8x8 HAS A SMALLER RATIO than 8x2x2?)

Future work includes using density functional theory with the minimum atom count determined by this study to negate finite-size effects.

ACKNOWLEDGMENTS

Thank you NERC

"We also acknowledge the use of high performance computing provided by Advanced Research Computing at the University of Leeds."

ANDREW HAS SOMETHING TO ADD (AMW IRF from NERC w/ grant code)

STEPHEN HAS SOMETHING TO ADD (LLSVP Grant from NERC / MSRC / ????)

---

[1] T. Lay, J. Hernlund, and B. A. Buffett, Nature Geoscience **1**, 25 (2008).

[2] J. M. Brown and R. G. McQueen, Journal of Geophysical Research **91**, 7485 (1986).

[3] M. Osako and E. Ito, Geophysical Research Letters **18**, 239 (1991).

[4] A. M. Hofmeister, Science **283**, 1699 (1999).

[5] A. F. Goncharov, P. Beck, V. V. Struzhkin, B. D. Haugen, and S. D. Jacobsen, Physics of the Earth and Planetary Interiors **174**, 24 (2009).

[6] G. M. Manthilake, N. de Koker, D. J. Frost, and C. A. McCammon, Proceedings of the National Academy of Sciences of the United States of America **108**, 1 (2011).

[7] K. Ohta, T. Yagi, N. Taketoshi, K. Hirose, T. Komabayashi, T. Baba, Y. Ohishi, and J. Hernlund, Earth and Planetary Science Letters **349-350**, 109 (2012).

[8] S. Stackhouse and L. Stixrude, Reviews in Mineralogy and Geochemistry **71**, 253 (2010).

[9] M. S. Green, The Journal of Chemical Physics **22**, 398 (1954).

[10] R. Kubo, Journa; of the Physical Society of Japan **12** (1957), 10.1143/JPSJ.12.570.

[11] R. Kubo, Reports on Progress in Physics **29**, 255 (1966).

[12] P. K. Schelling, S. R. Phillpot, and P. Keblinski, Physical Review B **65**, 144306 (2002).

[13] F. Muller-Plathe, The Journal of Chemical Physics **106**, 6082 (1997).

[14] C. Nieto-Draghi and J. B. Avalos, Molecular Physics **101**, 2303 (2013).

[15] D. P. Sellan, E. S. Landry, J. E. Turney, A. J. H. McGaughey, and C. H. Amon, Physical Review B **81**, 1 (2010).

[16] M. W. Ammann, A. M. Walker, S. Stackhouse, J. Wookey, A. M. Forte, J. P. Brodholt, and D. P. Dobson, Earth and Planetary Science Letters **390**, 175 (2014).

[17] S. Stackhouse, L. Stixrude, and B. B. Karki, Earth And Planetary Science Letters **427**, 11 (2015).

[18] V. Haigis, *Trace elements in silicate melts and the thermal conductivity of the earth's deep mantle: insights from atomistic modeling of geomaterials*, Ph.D. thesis, Freien Universität

Berlin (2013).

[19] X. Tang, M. C. Ntam, J. Dong, E. S. G. Rainey, and A. Kavner, Geophysical Research Letters **41**, 2746 (2014).

[20] H. Dekura, T. Tsuchiya, and J. Tsuchiya, Physical Review Letters **110**, 1 (2013).

[21] L. Hu, W. J. Evans, and P. Keblinski, Journal of Applied Physics **110**, 113511 (2011).

[22] J. A. Thomas, R. M. Iutzi, and A. J. H. McGaughey, Physical Review B - Condensed Matter and Materials Physics **81**, 1 (2010).

[23] S. Plimpton, Journal of Computational Physics **117**, 1 (1995).

[24] A. R. Oganov, J. P. Brodholt, and D. G. Price, Physics of the Earth and Planetary Interiors **122**, 277 (2000).

[25] P. C. Howell, The Journal of chemical physics **137**, 224111 (2012).

FIGURE CAPTIONS

FIG. 1. Idealised example of linear extrapolation procedure. Inverse computed conductivities are plotted against inverse simulation lengths. Extrapolation to y-axis gives conductivity of an infinite system length, i.e. the bulk material.

FIG. 2. Normalised ACF. Correlation is taken over a longer length than shown on this plot (10 ps, see Figure 8 below), however the function decays to less than 1% of its initial value at 2 ps. It continues to oscillate about zero, with a positive average value.

FIG. 3. Integrated ACF, multiplied by constants to get thermal conductivity. Large variation in the first 1 ps corresponds to the correlation time where the ACF is unconverged (still decaying / large oscillations). Thermal conductivity is averaged from correlation time of 5 ps - 10 ps (region in red box).

FIG. 4. CAPTION

FIG. 5. normalised acf in percent against 2ps correl

FIG. 6. kappa against 100ps correl

FIG. 7. kappa w/ uncertainty against 100ps correl

FIG. 8. kappa w/ uncertainty against 10ps correl

FIG. 9. kappa vs. volume, all directions

FIG. 10. The results of Figure 9 for cross-section of 2x2 and lengths 16 unit cells. Diagrams of cell geometry are shown, with dimensions in unit cells and the number of atoms. Green-Kubo result is plotted on the y-axis for comparison with extrapolated direct method conductivity.

FIG. 11. Compilation of direct method thermal conductivities across a range of cell shapes at 4000 K and static pressure of 136 GPa. Different cross-sections are displayed by the colour of the series, diagrams of which are shown in the legend (right). From right to left, data points correspond to lengths of 6, 8, 10, 12, 16, 24, and 48 unit cells. Inverted axes facilitate the extrapolation of conductivity to bulk material.

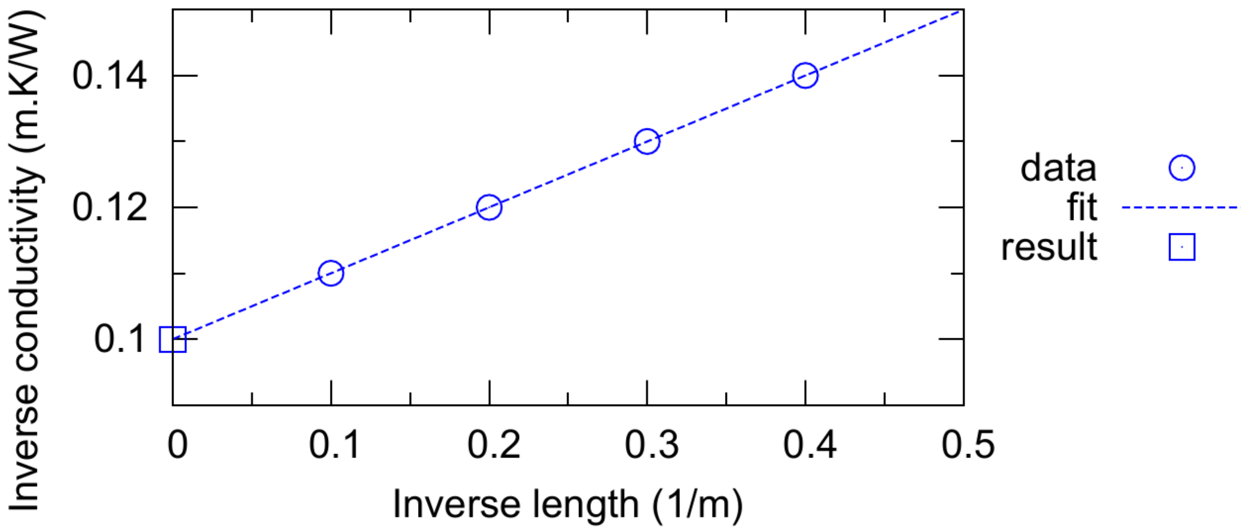

FIG. 1. Idealised example of linear extrapolation procedure. Inverse computed conductivities are plotted against inverse simulation lengths. Extrapolation to y-axis gives conductivity of an infinite system length, i.e. the bulk material.

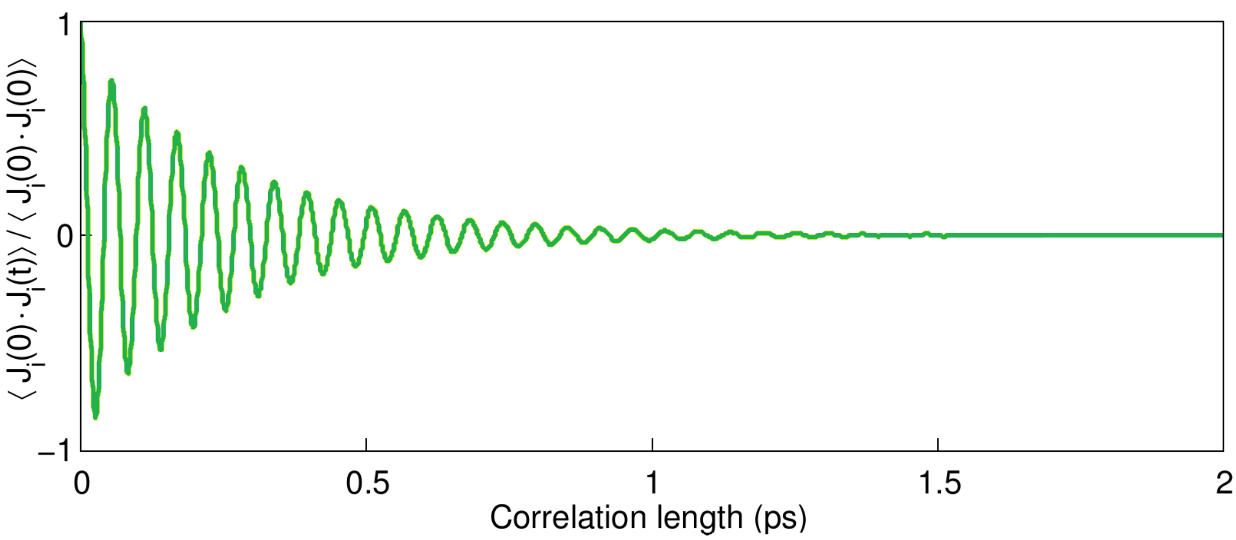

FIG. 2. Normalised ACF. Correlation is taken over a longer length than shown on this plot (10 ps, see Figure 8 below), however the function decays to less than 1% of its initial value at 2 ps. It continues to oscillate about zero, with a positive average value.

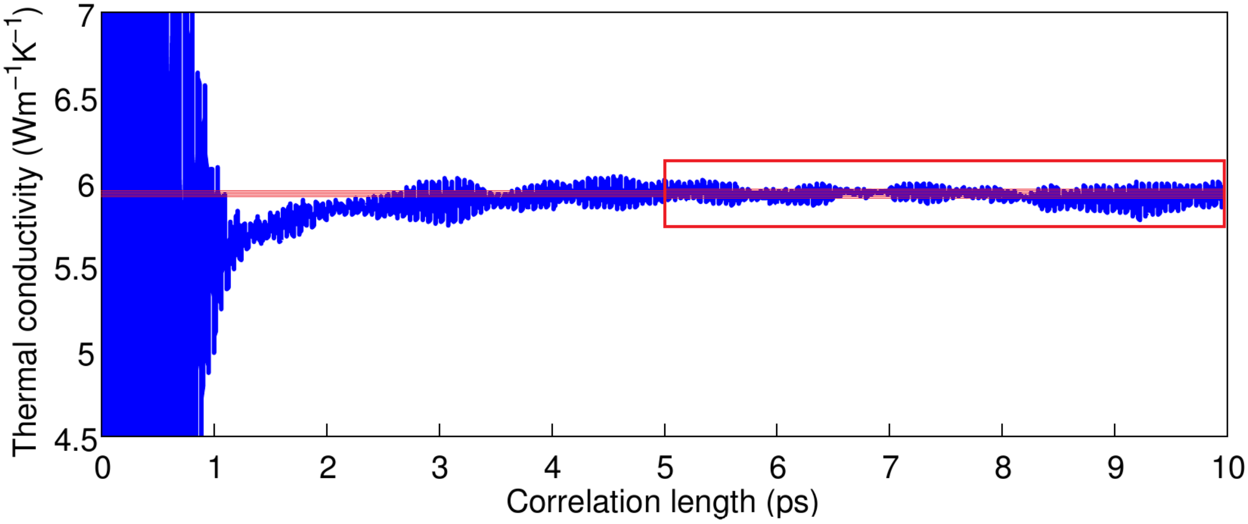

FIG. 3. Integrated ACF, multiplied by constants to get thermal conductivity. Large variation in the first 1 ps corresponds to the correlation time where the ACF is unconverged (still decaying / large oscillations). Thermal conductivity is averaged from correlation time of 5 ps - 10 ps (region in red box).

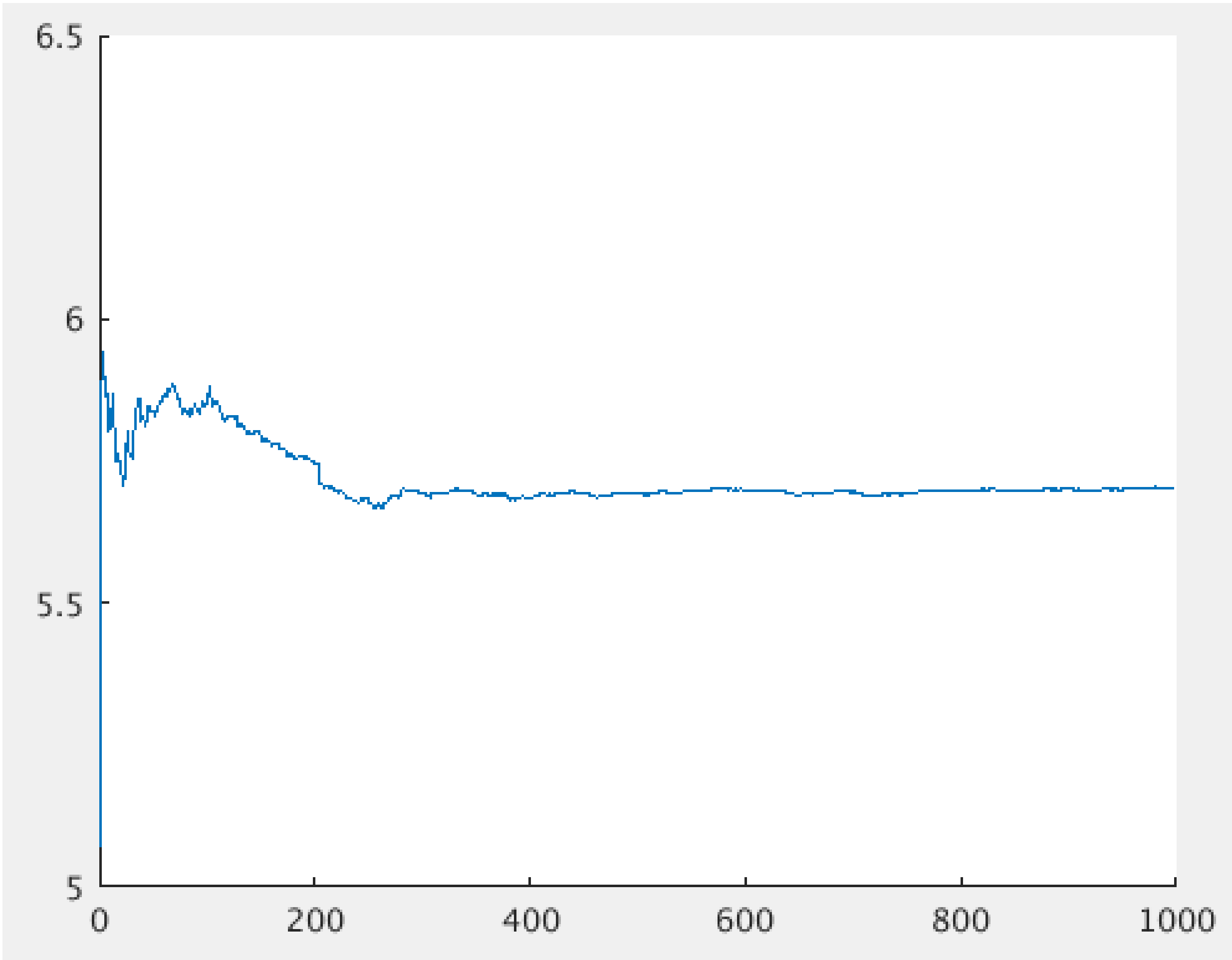

FIG. 4. CAPTION

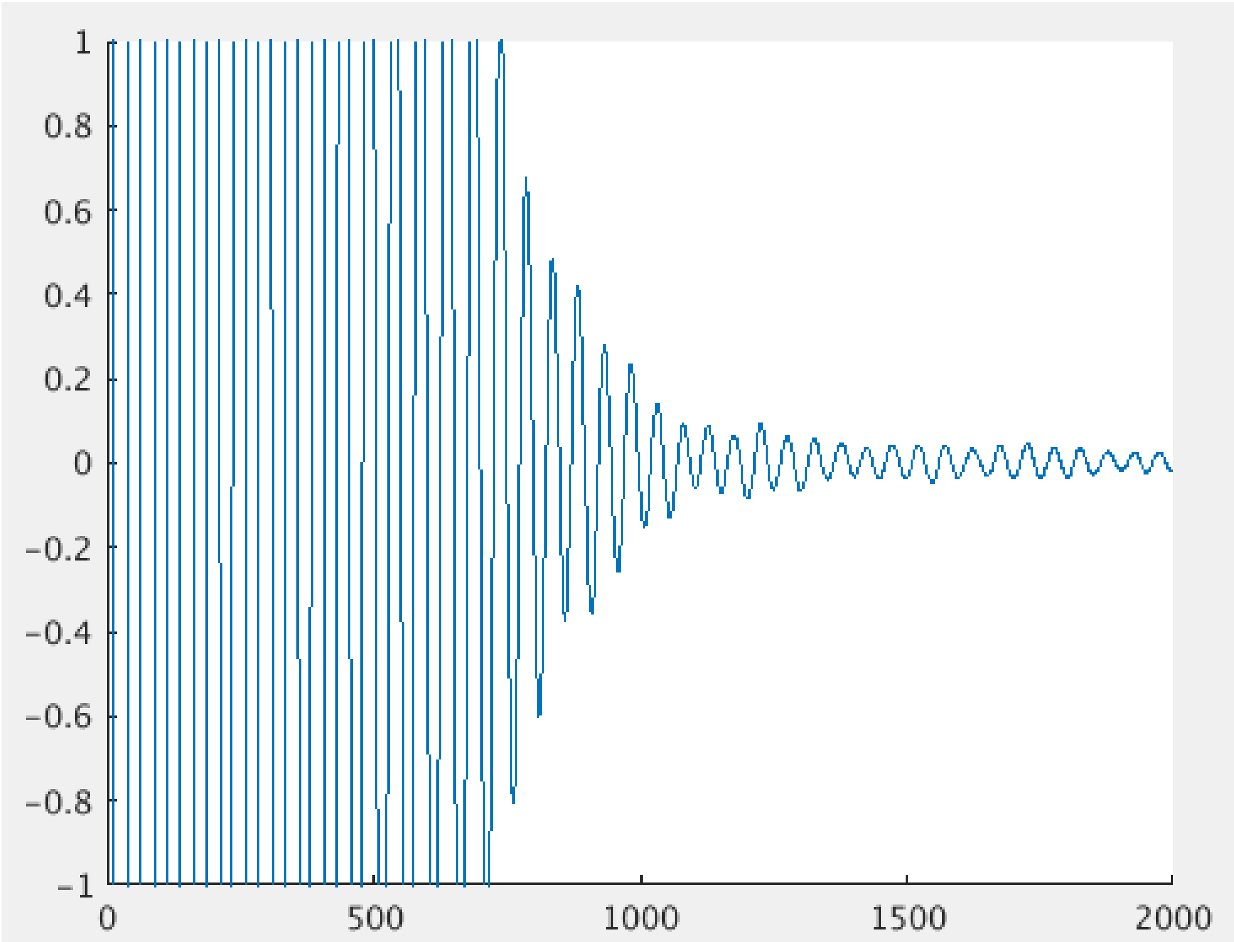

FIG. 5. normalised acf in percent against 2ps correl

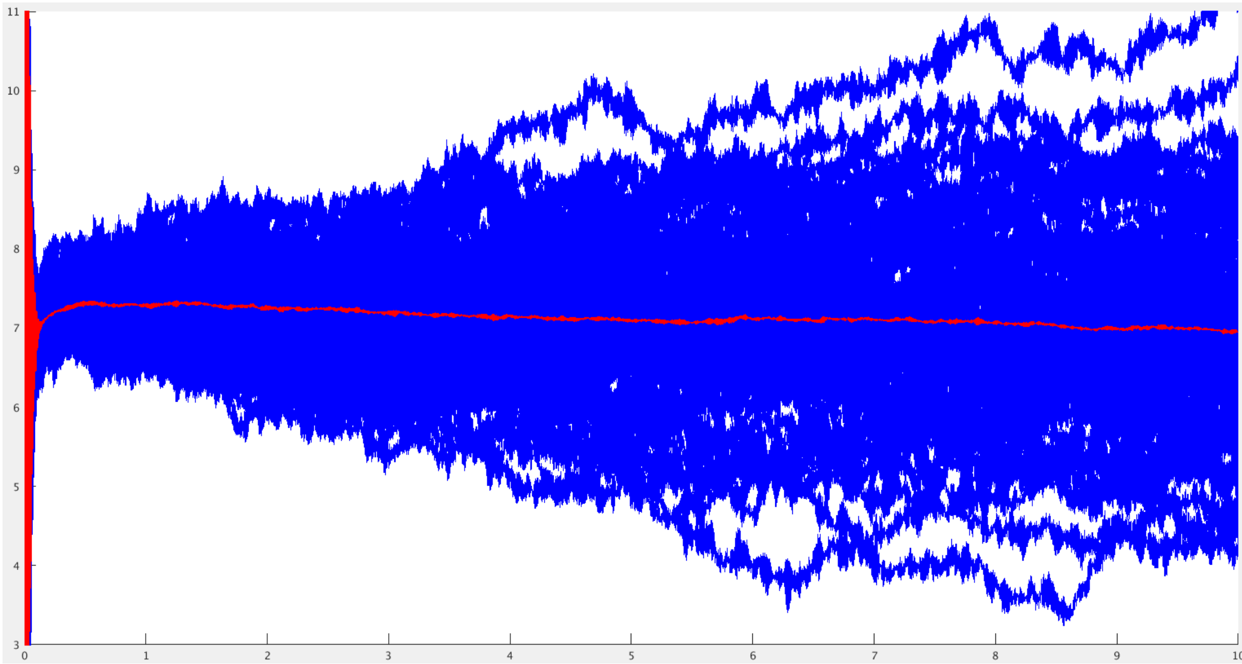

FIG. 6. kappa against 100ps correl

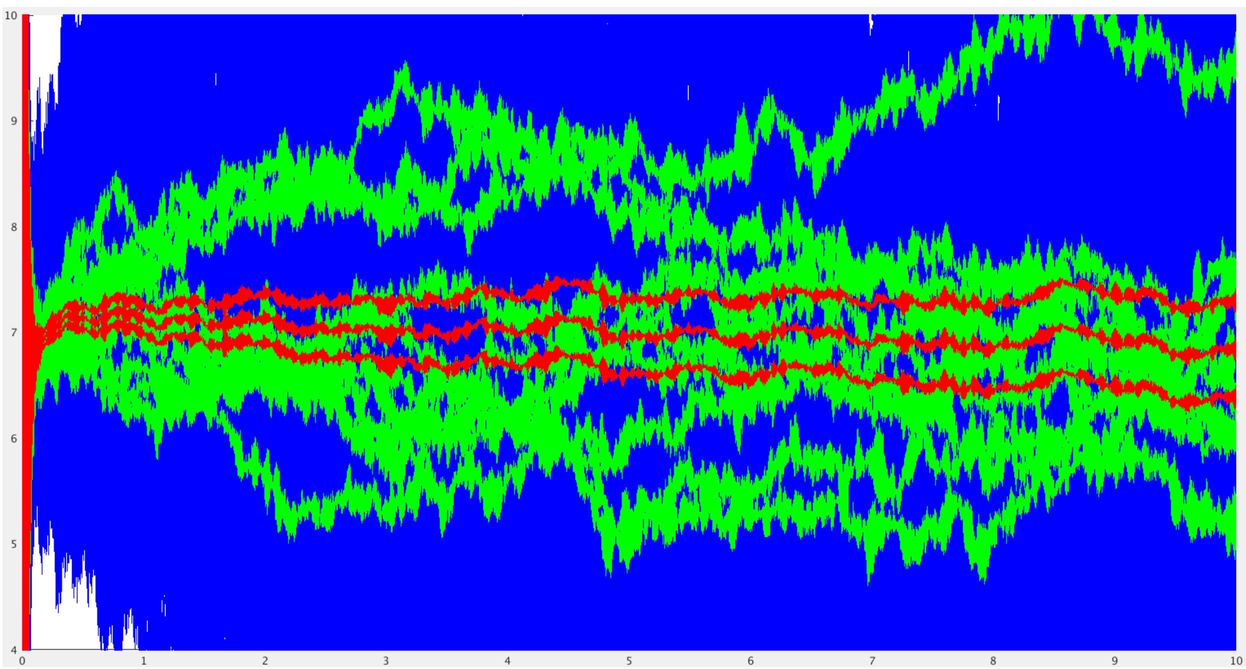

FIG. 7. kappa w/ uncertainty against 100ps correl

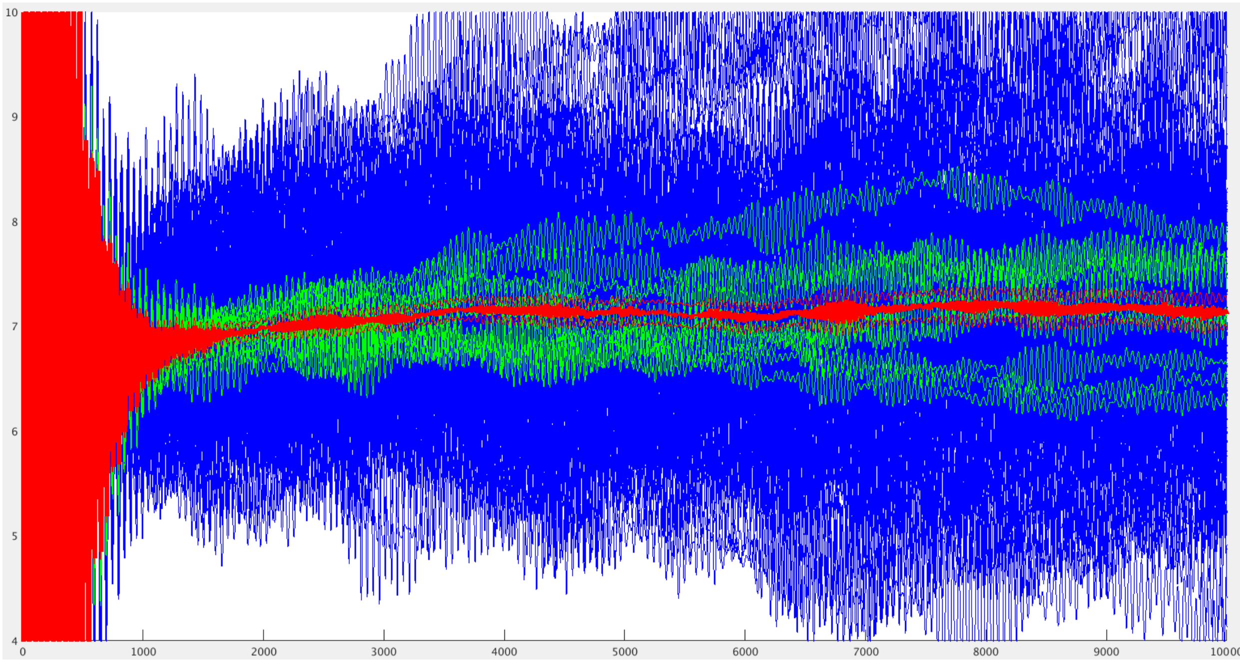

FIG. 8. kappa w/ uncertainty against 10ps correl

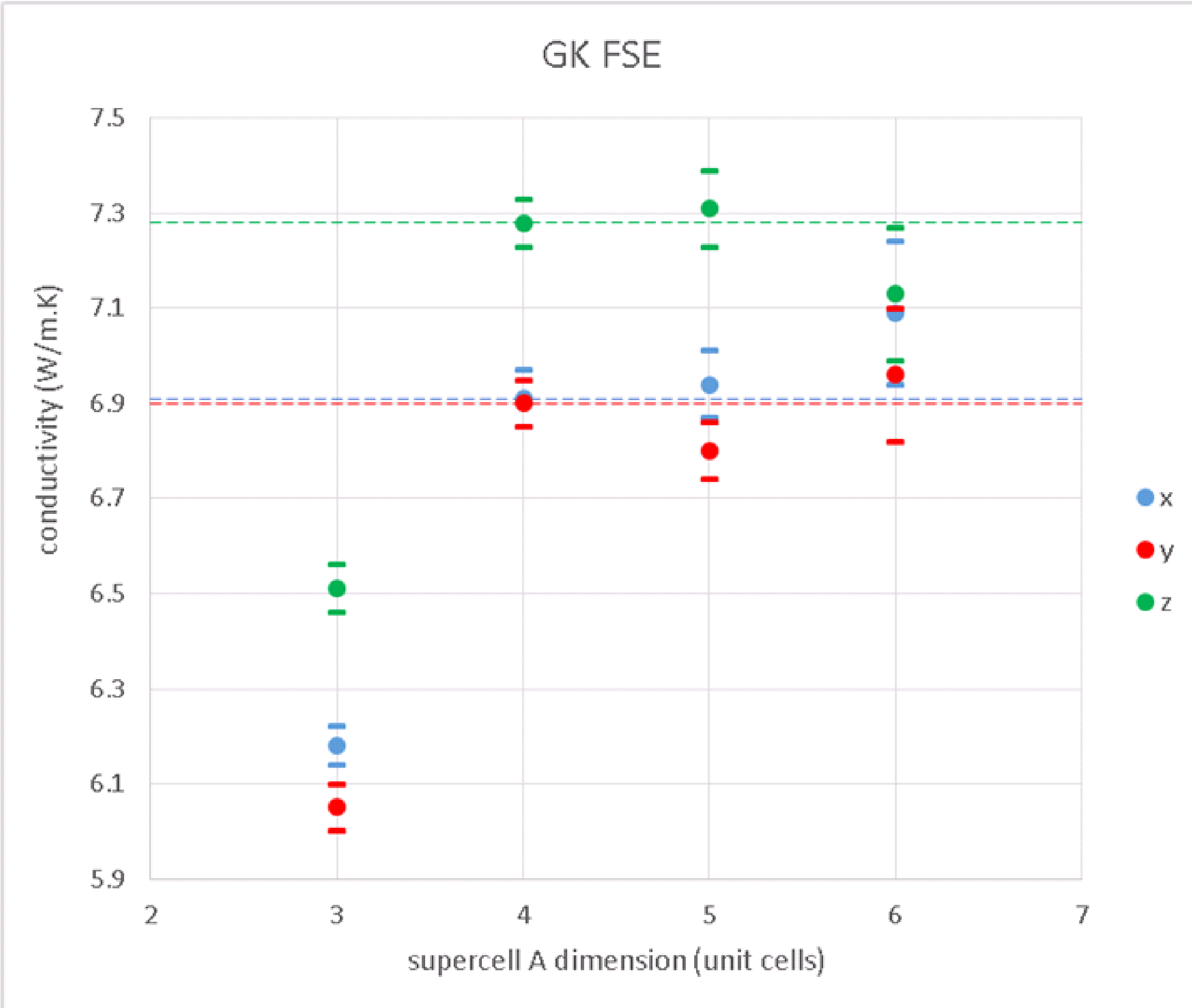

FIG. 9. kappa vs. volume, all directions

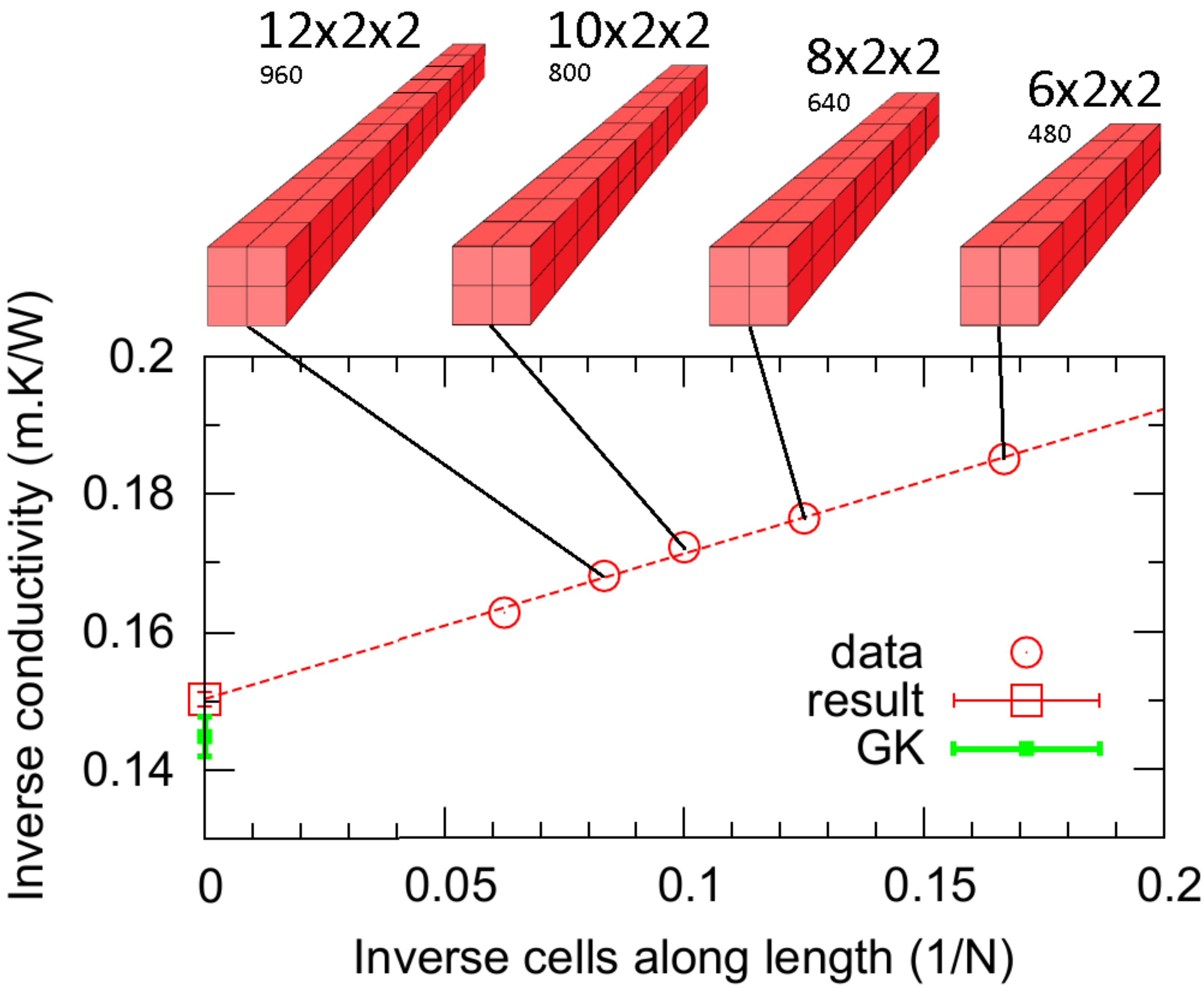

FIG. 10. The results of Figure 9 for cross-section of 2x2 and lengths 16 unit cells. Diagrams of cell geometry are shown, with dimensions in unit cells and the number of atoms. Green-Kubo result is plotted on the y-axis for comparison with extrapolated direct method conductivity.

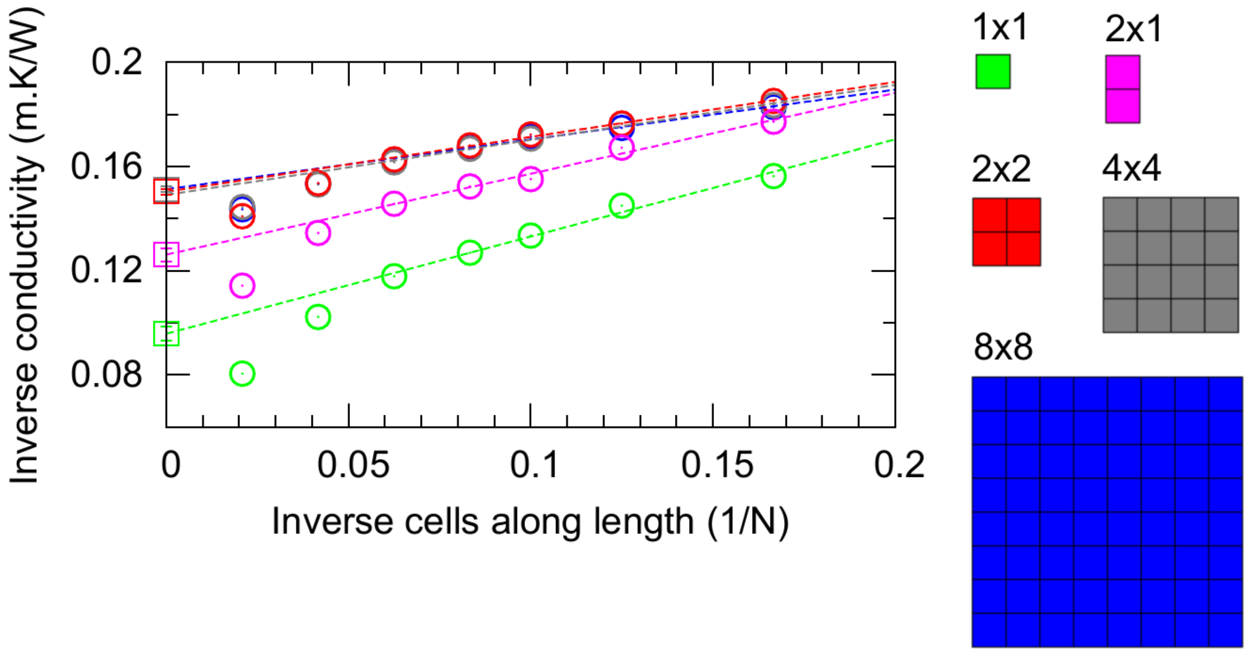

FIG. 11. Compilation of direct method thermal conductivities across a range of cell shapes at 4000 K and static pressure of 136 GPa. Different cross-sections are displayed by the colour of the series, diagrams of which are shown in the legend (right). From right to left, data points correspond to lengths of 6, 8, 10, 12, 16, 24, and 48 unit cells. Inverted axes facilitate the extrapolation of conductivity to bulk material.